Biochemical and Biophysical Research Communications 441 (2013) 726–731

Contents lists available at ScienceDirect

Biochemical and Biophysical Research Communications

journal homepage: www.elsevier.com/locate/ybbrc

Context-dependent role of ATG4B as target for autophagy inhibition in prostate cancer therapy

Elisa Tran [a], Annabelle Chow [a], Takeshi Goda [a], Amy Wong [a], Kim Blakely [a], Michelle Rocha [a], Samira Taeb [a], Van C. Hoang [a], Stanley K. Liu [a,b], Urban Emmenegger [a,c,*]

[a] Biological Sciences, Sunnybrook Research Institute, Canada
[b] Department of Radiation Oncology and Medical Biophysics, Odette Cancer Centre, Canada
[c] Division of Medical Oncology, Odette Cancer Centre, Sunnybrook Health Sciences Centre, University of Toronto, Toronto, ON, Canada

ARTICLE INFO

Article history:
Received 18 October 2013
Available online 30 October 2013

Keywords:
ATG4B
Autophagy
Prostate cancer
Chemotherapy
Radiation therapy

ABSTRACT

ATG4B belongs to the autophagin family of cysteine proteases required for autophagy, an emerging target of cancer therapy. Developing pharmacological ATG4B inhibitors is a very active area of research. However, detailed studies on the role of ATG4B during anticancer therapy are lacking. By analyzing PC-3 and C4-2 prostate cancer cells overexpressing dominant negative ATG4B^{C74A} *in vitro* and *in vivo*, we show that the effects of ATG4B^{C74A} are cell type, treatment, and context-dependent. ATG4B^{C74A} expression can either amplify the effects of cytotoxic therapies or contribute to treatment resistance. Thus, the successful clinical application of ATG4B inhibitors will depend on finding predictive markers of response.

1. Introduction

Macroautophagy (hereafter referred to as autophagy) is an evolutionarily conserved process implicated in cellular homeostasis and response to stress [1,2]. Briefly, cellular macromolecules or organelles are sequestered in autophagosomes, which in turn fuse with lysosomes to form autolysomes. The activation of lysosomal enzymes then mediates the degradation of the autolysosome content to procure cells with carbohydrates, nucleotides, amino acids, and fatty acids. By enabling the removal of damaged cellular components, and by providing building blocks for anabolic reactions or energy production, autophagy can contribute to cell survival. Conversely, unabated autophagy has been associated with cell death, although it is controversial if autophagy is a bona fide mechanism of cell death on its own [3].

While autophagy plays an important role in a broad range of disease conditions, its role in cancer is particularly complex [1,4]. During early carcinogenesis the tumor suppressing activities of autophagy seem to prevail (e.g., mitigation of DNA damage). In contrast, autophagy may contribute to tumor cell survival in established tumors that are commonly characterized by severe hypoxia and reduced nutrient availability, and in tumors subjected to cytotoxic therapy. Therefore, autophagy inhibition is being studied in phase II clinical trials combining the autophagy inhibitor hydroxychloroquine with chemotherapy (www.clinicaltrials.gov) [5].

Hydroxychloroquine is a lysosomotropic 4-aminoquinoline that impairs the fusion of autophagosomes and lysosomes, and that inhibits the acidification of autolysosomes and thus lysosomal enzyme activation [5–7]. However, the clinical development of hydroxychloroquine as an anticancer agent is challenging due to poor pharmacokinetic properties for cancer indications, lack of specificity, side-effects that could be enhanced by concomitant chemotherapy, and concerns whether the tissue levels of hydroxychloroquine that can be safely achieved are high enough to significantly impair autophagy [6,8,9]. Hence, the development of more potent and specific autophagy inhibitors is a very active area of research [10–15]. ATG4B (autophagy-related 4B, also named autophagin-1) is a particularly interesting drug target in this respect. ATG4B belongs to the autophagin family of cysteine proteases required for autophagy [16]. By controlling the lipidation status of the autophagosome membrane protein LC3 (microtubule-associated protein 1 light chain 3), ATGB4 controls autophagosome maturation. Briefly, pro-LC3 is cleaved by ATG4B to its LC3-I isoform (18 kDa), followed by ATG7 and ATG3 mediated conjugation of LC3-I with phopshatidyl-ethanolamine to yield LC3-II (16 kDa), which integrates into the crescent autophagosome double-membrane under the control of the ATG5–ATG12–ATG16L complex [17]. Autophagic activity can be semi-quantified by obtaining the LC3-II/LC3-I ratio under steady state conditions, and by analyzing the LC3-II/LC3-I ratio as well as the accumulation of LC3-II in the presence of chloroquine, which inhibits the degradation of LC3-II.

* Corresponding author at: Sunnybrook Research Institute, Sunnybrook Health Sciences Centre T2-054, 2075 Bayview Avenue, Toronto, ON M4N3M5, Canada. Fax: +1 416 480 6002.
E-mail address: urban.emmenegger@sunnybrook.ca (U. Emmenegger).

0006-291X/$ - see front matter © 2013 Elsevier Inc. All rights reserved.
http://dx.doi.org/10.1016/j.bbrc.2013.10.117

The latter reveals information about the autophagic flux [18]. The protease activity of ATG4B is considered more readily druggable than the complex protein–protein interactions found in other components of the autophagy machinery such as the multi-protein autophagy initiation complex. Furthermore, one expects ATG4B inhibitors to be very well tolerated given that the phenotype of *atg4b* deficient mice is largely restricted to inner ear development abnormalities [19,20].

Given the lack of detailed studies on the role of ATG4B during anticancer therapy [21], we describe herein the derivation of PC-3 and C4-2 prostate cancer cells expressing ATG4B^{C74A}, a dominant negative mutant of ATG4B phenocopying the characteristics of *atg4b* deficient cells [19,22].

2. Materials and methods

2.1. Materials

Docetaxel (Sanofi) and doxorubicin (Novopharm) were obtained from the Odette Cancer Centre Pharmacy. Docetaxel was freshly reconstituted before each use as per manufacturer's instructions. Doxorubicin saline stock solution was kept at 4 °C. Topotecan (gift of Dr. R.S. Kerbel) was reconstituted in DMSO and the stock solution was kept at −80 °C. All other reagents were obtained from Sigma–Aldrich unless otherwise indicated.

2.2. Cell lines and culturing

PC-3 (purchased from the American Type Culture Collection) and C4-2 (gift from Dr. M. Gleave) human prostate cancer cells were maintained in Dulbecco's Modified Eagle Medium (DMEM; high glucose with L-glutamine media, HyClone Laboratories) supplemented with 5% (v/v) fetal bovine serum (FBS; HyClone Laboratories) at 37 °C in a humidified atmosphere containing 5% CO_2. For autophagic flux studies, saturating concentrations of chloroquine (20 μM for both cell lines; Reyes, and Emmenegger, unpublished data) were added for the last 6 h of incubation.

For retrovirus production, we transfected HEK293T cells with pmStrawberry C1 or pmStrawberry-Atg4B^{C74A} (Addgene), envelop plasmid (VSV-G), and packaging plasmid (GAG-POL) using Lipofectamine 2000 (Life Technologies). PC-3 and C4-2 cells were transduced overnight in the presence of 10 μg/mL polybrene, and grown until sub-confluency before cell sorting (2 rounds) to obtain pools with high transgene expression.

2.3. Western blotting

Cell lysates were prepared in 25 mM Tris–HCl (pH 7.6), 150 mM NaCl, 1% NP-40, 1% sodium deoxycholate, 0.1% sodium dodecyl sulphate (SDS), and protease inhibitors (Complete, Mini Protease Inhibitor Cocktail Tablets, Roche Diagnostics), and separated on an SDS–polyacrylamide gel (15% for LC3 Western blots, 12% for ATG4B Western blots) before transfer onto PVDF (Polyvinylidene Fluoride) membranes (Millipore). The membranes were incubated with the following primary antibodies as indicated: anti-β-actin, anti-ATG4B, and anti-LC3B (Novus Biologicals). They were developed with a 1:10,000 dilution of horseradish peroxidase (HRP) conjugated secondary antibody (Stressgen) and the bands visualized with Western HRP Substrate Reagent (Millipore). For LC3 densitometry analyses, the LC3 values were automatically corrected by subtracting the background noise and normalized using β-actin. The ratio of LC3 II to LC3 I was calculated using the normalized values.

2.4. MTS proliferation assays

1×10^3 PC-3 cells per well and 1.5×10^3 C4-2 cells per well were seeded in 96-well plates in 50 μL of DMEM 5% FBS overnight. Thereafter, 50 μL of drug-containing culture media were added. After 72 h of incubation, the number of viable cells was quantified by applying the MTS assay (CellTitre 96® AQ_{ueous} Cell Proliferation Assay, Promega Corporation) according to the manufacturer's instructions.

2.5. Clonogenic survival assays

Mock irradiated cells, or cells irradiated with 2, 4, or 6 Gy, respectively, were subjected to clonogenic survival studies as previously described [23].

2.6. Animal procedures

All animal procedures were performed according to institutionally approved animal care guidelines (Sunnybrook Research Institute Animal Care Committee). 2×10^6 PC-3 cells were injected subcutaneously into the flanks of 6–8 week old, 25–30 g male athymic nude mice (Harlan). Tumor size was assessed weekly using calipers and by applying the formula ($0.5 \times [L \times W^2]$), where L and W represent the largest and the smallest tumor diameter, respectively. We also obtained serial mouse body weights as a measure of treatment toxicity. Doxorubicin (bolus of 6 mg/kg) was administered intraperitoneally once the tumors reached an average size of around 250 mm^3.

The tumor take rate and growth properties of C4-2 cells are considerably variable in athymic nude mice (Chow and Emmenegger, unpublished observations). Therefore, C4-2 cells were grown instead in severe-combined immunodeficient (SCID) mice harboring the ubiquitously expressed YFP (yellow fluorescent protein) transgene (in-house breeding program) [24]. 5×10^6 cells per mouse suspended in 50:50 (v/v) DMEM/Matrigel (BD Biosciences) were injected subcutaneously. We administered the maximum tolerated doxorubicin dose for SCID mice (2 mg/kg intraperitoneal bolus) once the tumors were established (i.e., around 250 mm^3) [25].

2.7. Statistical analyses

Results are reported as mean ± standard error of the mean unless otherwise indicated. Statistical significance of observed differences was assessed using GraphPad Prism Version 4.00. A p-value of less than 0.05 was considered significant.

3. Results

3.1. Characterization of ATG4B^{C74A} expressing PC-3 and C4-2 human prostate cancer cell lines

Following transduction with pmStrawberry-Atg4b^{C74A}, we found a ratio of ATG4B^{C74A} over endogenous ATG4B of around 2.5 (PC-3) and 3 (C4-2), which was not markedly affected by autophagy-promoting culture conditions such as hypoxia (1% O_2), or by chloroquine treatment (Fig. 1A, C). The presence of ATG4B^{C74A} considerably changed the expression pattern of LC3 isoforms (Fig. 1B/C, E/F). LC3-I was found to accumulate in ATG4B^{C74A} expressing PC-3 and C4-2 compared to corresponding control cells. When PC-3 cells were exposed to chloroquine to study autophagic flux, the LC3-II/LC3-I ratio decreased from 1.54 (PC-3mstr) to 1.05 (PC-3atg4b^{C74A}) under standard tissue culture conditions, indicating reduced basal autophagy (Fig. 1B). Under hypoxia induced autophagy (1% O_2), the difference of the LC3-II/LC3-I ratios was even more

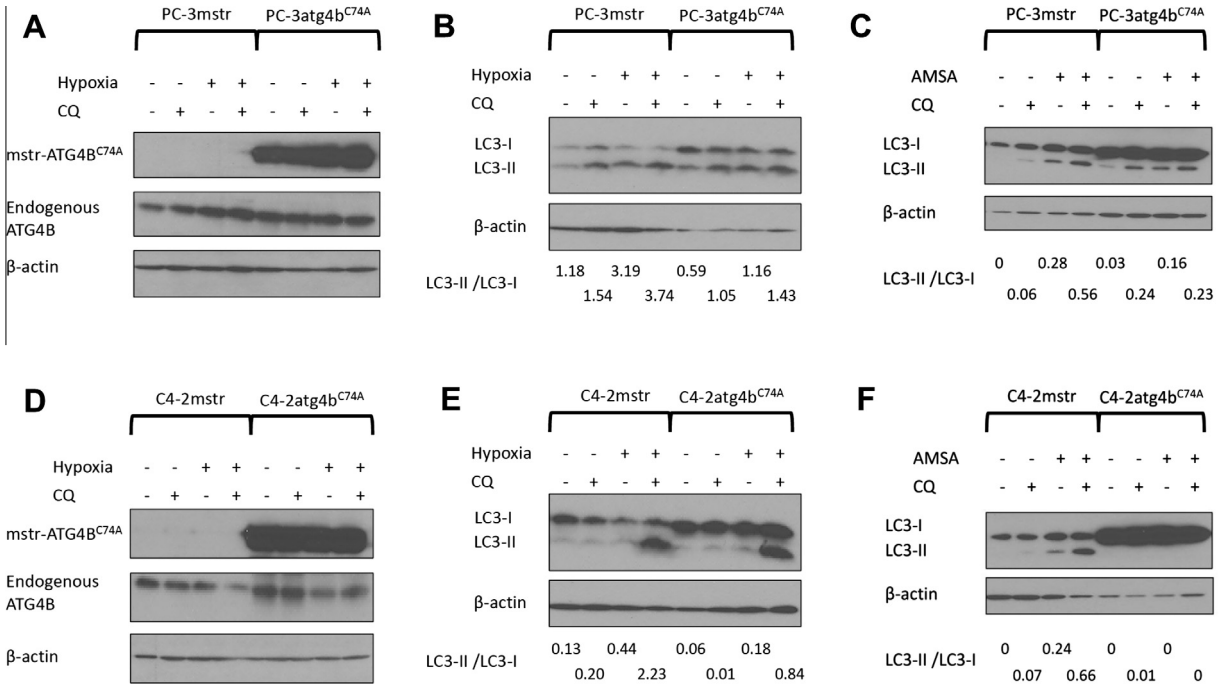

Fig. 1. Characterization of PC-3 and C4-2 human prostate cancer cell lines expressing ATG4B^{C74A}. (A) Retroviral transduction of PC-3 with pmStrawberry-Atg4b^{C74A} enabled marked expression of the mstrawberry-ATG4B^{C74A} fusion protein (mstr-ATG4B^{C74A}), which resulted in LC3-I accumulation and a lowered LC3-II/LC3-I ratio documenting impaired autophagy in PC-3atg4b^{C74A} exposed to metabolic (1% O_2 over 24 h) (B) or cytotoxic (amsacrine, AMSA; 10 μM) (C) stress when compared to control PC-3mstr cells transduced with pmStrawberry C1. (D) In ATG4B^{C74A} overexpressing C4-2, both hypoxia-induced (E) and amsacrine-induced autophagy (F) were even more impaired than in PC-3atg4B^{C74A}. CQ: chloroquine (20 μM, added for the last 6 h of incubation).

pronounced (3.74 versus 1.43). We observed similar changes in the C4-2 model (Fig. 1E).

To further characterize our cell models we also used amsacrine, a topoisomerase II inhibitor with particularly strong autophagy inducing properties [26]. In the presence of amsacrine, the LC3-II/LC3-I ratio was reduced in PC-3atg4b^{C74A} compared to PC-3mstr (Fig. 1C). As per LC3-II/LC3-I ratio, the autophagic flux was 2-fold lower in PC-3atg4b^{C74A} versus PC-3mstr (0.23 versus 0.56). In C4-2atg4b^{C74A}, LC3-II was undetectable (Fig. 1F).

3.2. Differential impact of ATG4B^{C74A} on in vitro chemosensitivity of PC-3 versus C4-2

Given their frequent use in the treatment of advanced prostate cancer, we studied the antiproliferative effects of docetaxel (taxane microtubule inhibitor) and of doxorubicin (intercalating topoisomerase II inhibitor) by applying MTS assays in PC-3mstr versus PC-3atg4b^{C74A}, and in C4-2mstr versus C4-2atg4b^{C74A} (Table 1A). Of note, MTS assay data highly correlate with conventional cell counting in both ATG4B^{C74A} expressing and control cells, although the MTS assay is based on mitochondrial enzymatic activity, which could be affected by the autophagy status (Supplemental Fig. S1). Overall, PC-3 cells were more resistant to docetaxel than C4-2 cells (Fig. 2A, D). Otherwise, neither PC-3atg4b^{C74A} nor C4-2atg4b^{C74A} differed significantly in their response to docetaxel when compared to PC-3mstr or C4-2mstr.

The half maximal inhibitory concentration (IC_{50}) of doxorubicin for PC-3mstr was around 2-fold higher compared to C4-2mstr (0.066 versus 0.032 μg/mL) (Table 1A). However, ATG4B^{C74A} expression resulted in opposite effects in PC-3 versus C4-2 (Fig. 2B, E). While the doxorubicin IC_{50} for PC-3atg4b^{C74A} was moderately but significantly increased compared to PC-3mstr (i.e., by 25%), ATG4B^{C74A} expression markedly sensitized C4-2 to the effects of doxorubicin by around 4-fold (Table 1A). To expand on the findings with doxorubicin, we also tested the topoisomerase I inhibitor topotecan to see the same phenomenon. ATG4B^{C74A} expression promoted resistance to topotecan in PC-3 yet chemosensitized C4-2 (Fig. 2C, F). Supplemental Fig. S2 summarizes the relative changes of docetaxel, doxorubicin, or topotecan IC_{50}'s in ATG4B^{C74A} expressing PC-3 or C4-2 cells compared to their corresponding control cells.

3.3. ATG4B^{C74A} amplifies radiation effects in C4-2 but promotes radiation resistance in PC-3

Since topoisomerase inhibition results in DNA double-strand breaks, we asked if the differential response of PC-3atg4b^{C74A} versus C4-2atg4b^{C74A} to doxorubicin and topotecan could be replicated by radiation-induced DNA damage. Indeed, clonogenic survival assays revealed the same response pattern (Supplemental Fig. S3). PC-3atg4b^{C74A} were more resistant to irradiation than

Table 1A
Half maximal inhibitory drug concentrations (IC_{50}).

	PC-3mstr	PC-3atg4b^{C74A}	*p*-value	C4-2mstr	C4-2atg4b^{C74A}	*p*-value
Docetaxel (mean ± SEM; ng/mL)	1.259 ± 0.025	1.260 ± 0.137	*0.991*	0.881 ± 0.020	0.827 ± 0.030	*0.226*
Doxorubicin (mean ± SEM; μg/mL)	0.066 ± 0.009	0.082 ± 0.007	*0.025*	0.032 ± 0.007	0.008 ± 0.001	*0.048*
Topotecan (mean ± SEM; μg/mL)	0.018 ± 0.002	0.043 ± 0.006	*0.024*	0.021 ± 0.005	0.006 ± 0.001	*0.042*

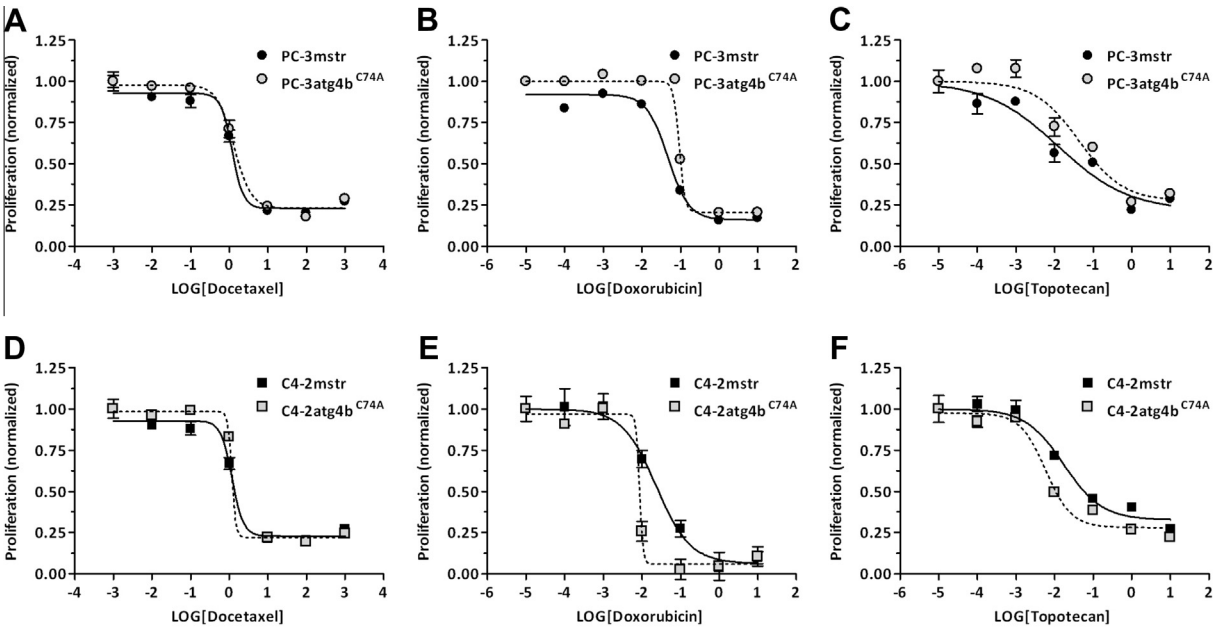

Fig. 2. Chemosensitivity studies. Cells were treated for 72 h with docetaxel (0.001–0.01–0.1–1–10–100–1000 ng/mL) (A, D), doxorubicin (0.00001–0.0001–0.001–0.01–0.1–1–10 μg/mL) (B, E) or topotecan (0.00001–0.0001–0.001–0.01–0.1–1–10 μg/mL) (C, F), followed by MTS assay. While the autophagy status did not affect proliferation of PC-3 cells exposed to docetaxel (A), ATG4B^{C74A} expression promoted resistance to both doxorubicin (B), and topotecan (C). On the other hand, ATG4B^{C74A} expression sensitized C4-2 to the antiproliferative effects of doxorubicin (E) and of topotecan (F), yet its effect was neutral with respect to docetaxel (D). One representative experiment out of ⩾3 independent experiments shown; $n = 3$ per datapoint.

Table 1B
Autophagy induction patterns.

	PC-3mstr Autophagy flux	PC-3 atg4b^{C74A} Autophagy flux	LC3-II/LC3-I ratio PC-3atg4b^{C74A}/PC-3mstr	C4-2mstr Autophagy flux	C4-2 atg4b^{C74A} Autophagy flux	LC3-II/LC3-I ratio C4-2atg4b^{C74A}/C4–2mstr
Docetaxel	↓	↓	↓	↑	Ø	↓↓
Doxorubicin	↑	↓	↓	↑	Ø	↓↓
Topotecan	↑	↔	↑	↑	Ø	↓↓

PC-3mstr, whereas ATG4B^{C74A} expression sensitized C4-2 to radiation therapy.

3.4. Differential chemotherapy-induced autophagy patterns in PC-3 versus C4-2 cells

Given the differential responses to doxorubicin and topotecan in the PC-3 versus C4-2 models, we wondered if this could be explained by model-dependent variations in chemotherapy-associated autophagy induction. Representative LC3 Western blots are shown in Supplemental Fig. S4, and the autophagy induction patterns are summarized in Table 1B. In C4-2mstr, all three chemotherapy drugs tested induced the autophagic flux. However, no discernible LC3-II conversion took place in C4-2atg4b^{C74A} (Fig. S4D–F). The response of PC-3mstr and PC-3atg4b^{C74A} to chemotherapy was more variable. While doxorubicin and topotecan modestly induced autophagy in PC-3mstr (Fig. S4B, C), both the steady-state LC3-II/LC3-I ratio and the autophagic flux were reduced by docetaxel (Fig. S4A). In contrast to C4-2atg4b^{C74A}, the conversion of LC3-I to LC3-II was not fully suppressed in PC-3atg4b^{C74A} exposed to chemotherapy. However, both docetaxel and doxorubicin treatment impaired the autophagic flux in PC-3atg4b^{C74A}, whereas the effects of topotecan were neutral (Fig. S4A–C). When comparing PC-3mstr with PC-3atg4b^{C74A}, the autophagic flux was around 3-fold lower in PC-3atg4b^{C74A} treated with docetaxel or doxorubicin, but was 2-fold greater in topotecan treated PC-3atg4b^{C74A}.

3.5. Doxorubicin therapy of PC-3 and C4-2 xenograft tumors does not replicate the findings of the proliferation assays

We wondered if the differential response of PC-3atg4b^{C74A} versus C4-2atg4b^{C74A} to doxorubicin *in vitro* would predict the *in vivo* behavior of corresponding xenograft tumors. The treatment of established PC-3mstr tumors (~250 mm^3) grown in athymic nude mice was not significantly affected by doxorubicin (Fig. 3A) at the well tolerated dose of 6 mg/kg (Fig. S5A). Although PC-3atg4b^{C74A} cells were found to be more resistant to doxorubicin *in vitro* than PC-3mstr, the growth of PC-3atg4b^{C74A} tumors was significantly impaired by doxorubicin (Fig. 3B). Of note, the growth pattern of PC-3mstr versus PC-3atg4b^{C74A} tumors was different. While the lag-phase to an approximate size of around 250 mm^3 was 5 weeks in PC-3mstr compared to 4 weeks in PC-3atg4b^{C74A} tumors, tumor progression beyond 250 mm^3 was accelerated in PC-3mstr compared to PC-3atg4b^{C74A} tumors.

C4-2mstr tumors reached an average size of around 250 mm^3 within 8 weeks (Fig. 3C), whereas the lag phase of C4-2atg4b^{C74A} tumors to 250 mm^3 was significantly shorter (around 2 weeks) and followed by rapid tumor expansion (Fig. 3D). The growth of C4-2mstr tumors was significantly impaired by doxorubicin (Fig. 3C). In contrast, despite 4-fold increased *in vitro* sensitivity of C4-2atg4b^{C74A} cells to doxorubicin compared to C4-2mstr, C4-2atg4b^{C74A} tumors were unresponsive to doxorubicin. As evidenced by serial body weight measurements, SCID mice tolerated doxorubicin at the 2 mg/kg dose reasonably well (Fig. S5C, D).

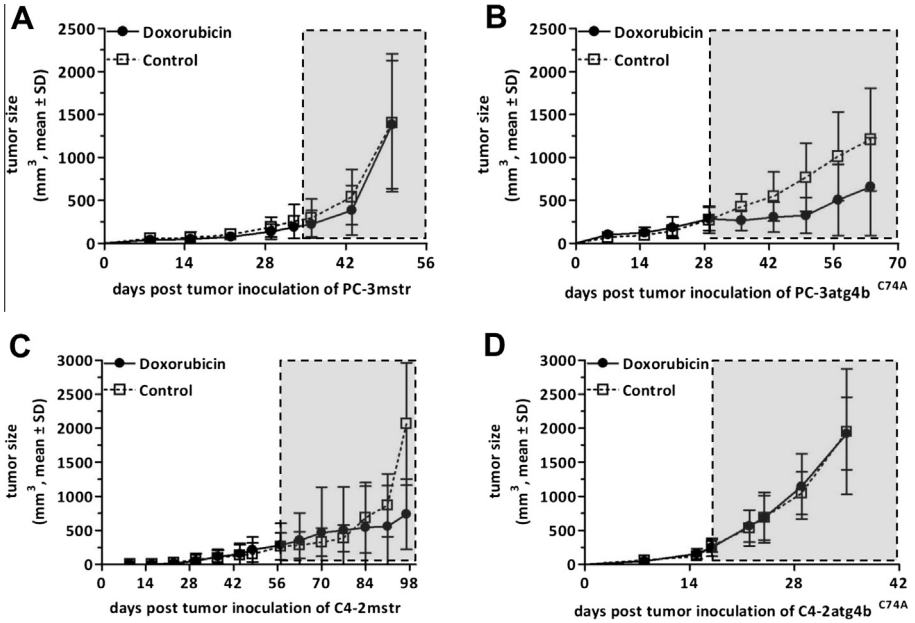

Fig. 3. Doxorubicin therapy of PC-3 and C4-2 tumor xenografts. (A) Established PC-3mstr tumors were found to be resistant to doxorubicin treatment (6 mg/kg), whereas the growth of (B) PC-3atg4b^{C74A} tumors was significantly inhibited ($p < 0.05$ day 49, and 56, *T*-test). Established PC-3atg4b^{C74A} tumors also displayed a less aggressive growth pattern than PC-3mstr. (C) C4-2mstr growth was significantly impaired by doxorubicin ($p < 0.05$ day 97, *T*-test). (D) In contrast, C4-2atg4b^{C74A} tumors were completely resistant to doxorubicin therapy and showed a more aggressive growth pattern than C4-2mstr. Shaded boxes: doxorubicin treatment period.

4. Discussion

Autophagy plays a dual role in therapeutic resistance, one of the major challenges of systemic anticancer therapy. By facilitating the removal of damaged cellular structures, and by supporting anabolic and repair processes in cells exposed to cytotoxic stress, autophagy can contribute to cell survival and thus to therapeutic resistance. On the other hand, autophagy may also contribute to cell death and hence to treatment response [4].

The dual role of autophagy is only one of the challenges in the clinical translation of autophagy modulation as an anticancer treatment strategy. There is also a lack of pharmacodynamic markers of autophagy for clinical purposes [27]. In addition, given limited single-agent activity, autophagy modulators are usually combined with other treatment modalities. However, there is a paucity of preclinical guidance with respect to defining the most promising treatment combinations. Clinically, the most advanced autophagy inhibitor to date, hydroxychloroquine, has pharmacokinetic as well as pharmacodynamic shortcomings and lacks specificity [6,8,9]. In contrast, the cysteine protease ATG4B is considered an autophagy-specific drug target. Furthermore, protease inhibitors have already been developed successfully for other disease conditions such as the human immunodeficiency virus infection [28]. While ATG4B inhibitors are being developed [11], the specific role of ATG4B in cancer and cancer therapy has not yet been widely studied. Apel et al. showed a radiation dose-dependent increase of *atg4b* mRNA expression in a panel of breast (MDA-MB-231), pharyngeal (HTB43), cervical (HTB35), and lung cancer (A549) cell lines [21]. On the other hand, *atg4b* RNA interference coincided with reduced clonogenicity following radiation therapy of HTB43 and MDA-MB-231, had no impact in HTB35 and increased the clonogenicity of A549. To the best of our knowledge, we are the first to study the role of ATG4B during chemotherapy, both *in vitro* and *in vivo*. We found both quantitative and qualitative differences in how PC-3 and C4-2 human prostate cancer cell lines are affected by the expression of dominant negative ATG4B^{C74A}.

First, ATG4B^{C74A} affects autophagy more markedly in C4-2 cells compared to PC-3 despite similar expression levels. A number of explanations could account for this difference, such as differential capability to bypass ATG4B inhibition by compensatory use of other ATG4 protease family members. In fact, although ATG4B is considered the most important ATG4 protease, the ATG4 family comprises 3 other members, albeit with different substrate specificities [16]. The consequences of ATG4B^{C74A} expression may also be modified by cell-type specific oncogene or suppressor gene alterations known to affect autophagy [29], or by genetic alterations of core autophagy genes [30].

Second, ATG4B^{C74A} expression sensitized C4-2 cells to doxorubicin, topotecan, and radiation *in vitro*. However, no such sensitization was seen in C4-2 treated with docetaxel. Altogether, our findings suggest that autophagy exerts cytoprotective functions in C4-2 experiencing DNA damage. In contrast, PC-3atg4b^{C74A} cells are more resistant to doxorubicin, topotecan, and radiation compared to PC-3mstr. Although one may argue that the more pronounced autophagy defect seen in C4-2 atg4b^{C74A} compared to PC-3 atg4b^{C74A} might account for the discrepancies seen, this would not explain all the discordant findings. In fact, while docetaxel induced autophagy in C4-2mstr but reduced the autophagic flux in PC-3mstr, neither C4-2atg4b^{C74A} nor PC-3atgb^{C74A} were significantly sensitized to the effects of docetaxel compared to corresponding control cells. On the other hand, PC-3 and C4-2 differ in their *p53* status (PC-3 cells are *p53* null, C4-2 cells express wildtype *p53*), which may affect the implications of autophagy modulation [29]. The neutral effects of ATG4B^{C74A} expression in the context of docetaxel therapy are not completely unexpected. Recent compound screening suggests that most microtubule inhibitors are unlikely to induce autophagy [26], yet can interfere with the fusion of autophagosomes with lysosomes and thus exert anti-autophagic effects [31,32]. Therefore, reducing autophagy even further in microtubule inhibitor exposed tumor cells may have more modest biological consequences compared to obliterating the massive autophagic reaction associated with topoisomerase inhibition [26].

Third, *in vitro* proliferation assays with doxorubicin do not predict the response to doxorubicin *in vivo*. In fact, the *in vitro* versus *in vivo* response patterns of C4-2atg4b^{C74A} compared to C4-2mstr, and of PC-3atg4b^{C74A} versus PC-3mstr, were reversed. Current

investigations are aiming at understanding these discordant findings. Notably, the *in vivo* use of doxorubicin is associated with antitumor effects that cannot be accounted for *in vitro* (e.g., antivascular effects and associated metabolic stress [33]), but that may have an impact on the role of autophagy for tumor cell survival.

Fourth, ATG4B^{C74A} overexpression changes the growth characteristics in both tumor models. The aggressive growth behavior of C4-2atg4b^{C74A} is not without precedent [34] but concerning regarding the clinical use of autophagy inhibitors, including ATG4B inhibitors.

Our results position ATG4B inhibition as an alternative strategy to lysosomotropic therapy. At the same time, they also point to the challenges of clinically developing autophagy inhibitors as anticancer agents. To bring the right drug to the right patient at the right time, we will need both predictive markers of response and pharmacodynamic markers of autophagic activity. The cell models described herein are a very promising tool to study the molecular mechanisms of the differential responses to chemotherapy and radiation seen, and to ultimately identify predictive markers of response.

Acknowledgments

We are grateful to Dr. M.M. Rahim Mobin for providing us with the retroviral transduction system. These studies were conducted with funds from Prostate Cancer Canada to U. Emmenegger.

Appendix A. Supplementary data

Supplementary data associated with this article can be found, in the online version, at http://dx.doi.org/10.1016/j.bbrc.2013.10.117.

References

[1] A.M. Choi, S.W. Ryter, B. Levine, Autophagy in human health and disease, N. Engl. J. Med. 368 (2013) 651–662.
[2] G. Kroemer, G. Marino, B. Levine, Autophagy and the integrated stress response, Mol. Cell. 40 (2010) 280–293.
[3] S. Shen, O. Kepp, G. Kroemer, The end of autophagic cell death?, Autophagy 8 (2012) 1–3
[4] E. White, Deconvoluting the context-dependent role for autophagy in cancer, Nat. Rev. Cancer 12 (2012) 401–410.
[5] Z.J. Yang, C.E. Chee, S. Huang, F.A. Sinicrope, The role of autophagy in cancer: therapeutic implications, Mol. Cancer Ther. 10 (2011) 1533–1541.
[6] Q. McAfee, Z. Zhang, A. Samanta, S.M. Levi, X.H. Ma, S. Piao, J.P. Lynch, T. Uehara, A.R. Sepulveda, L.E. Davis, J.D. Winkler, R.K. Amaravadi, Autophagy inhibitor Lys05 has single-agent antitumor activity and reproduces the phenotype of a genetic autophagy deficiency, Proc. Natl. Acad. Sci. U.S.A. 109 (2012) 8253–8258.
[7] V.R. Solomon, H. Lee, Chloroquine and its analogs: a new promise of an old drug for effective and safe cancer therapies, Eur. J. Pharmacol. 625 (2009) 220–233.
[8] J. Ducharme, R. Farinotti, Clinical pharmacokinetics and metabolism of chloroquine. Focus on recent advancements, Clin. Pharmacokinet. 31 (1996) 257–274.
[9] T. Kimura, Y. Takabatake, A. Takahashi, Y. Isaka, Chloroquine in cancer therapy: a double-edged sword of autophagy, Cancer Res. 73 (2013) 3–7.
[10] C.W. Shu, C. Madiraju, D. Zhai, K. Welsh, P. Diaz, E. Sergienko, R. Sano, J.C. Reed, High-throughput fluorescence assay for small-molecule inhibitors of autophagins/Atg4, J. Biomol. Screen. 16 (2011) 174–182.
[11] S.M. Gorski, J. Ries, J.J. Lum, Targeting autophagy: the Achilles' heel of cancer, Autophagy 8 (2012) 1279–1280.
[12] E. Donohue, A. Tovey, A.W. Vogl, S. Arns, E. Sternberg, R.N. Young, M. Roberge, Inhibition of autophagosome formation by the benzoporphyrin derivative verteporfin, J. Biol. Chem. 286 (2011) 7290–7300.
[13] S. Miller, B. Tavshanjian, A. Oleksy, O. Perisic, B.T. Houseman, K.M. Shokat, R.L. Williams, Shaping development of autophagy inhibitors with the structure of the lipid kinase Vps34, Science 327 (2010) 1638–1642.
[14] J. Liu, H. Xia, M. Kim, L. Xu, Y. Li, L. Zhang, Y. Cai, H.V. Norberg, T. Zhang, T. Furuya, M. Jin, Z. Zhu, H. Wang, J. Yu, Y. Li, Y. Hao, A. Choi, H. Ke, D. Ma, J. Yuan, Beclin1 controls the levels of *p53* by regulating the deubiquitination activity of USP10 and USP13, Cell 147 (2011) 223–234.
[15] D.C. Rubinsztein, P. Codogno, B. Levine, Autophagy modulation as a potential therapeutic target for diverse diseases, Nat. Rev. Drug Discov. 11 (2012) 709–730.
[16] A. Till, S. Subramani, A balancing act for autophagin, J. Clin. Invest. 120 (2010) 2273–2276.
[17] S.W. Ryter, S.J. Lee, A. Smith, A.M. Choi, Autophagy in vascular disease, Proc. Am. Thorac. Soc. 7 (2010) 40–47.
[18] D.J. Klionsky, F.C. Abdalla, H. Abeliovich, et al., Guidelines for the use and interpretation of assays for monitoring autophagy, Autophagy 8 (2012) 445–544.
[19] G. Marino, A.F. Fernandez, S. Cabrera, Y.W. Lundberg, R. Cabanillas, F. Rodriguez, N. Salvador-Montoliu, J.A. Vega, A. Germana, A. Fueyo, J.M. Freije, C. Lopez-Otin, Autophagy is essential for mouse sense of balance, J. Clin. Invest. 120 (2010) 2331–2344.
[20] R. Read, K. Savelieva, K. Baker, G. Hansen, P. Vogel, Histopathological and neurological features of ATG4B knockout mice, Vet. Pathol. 48 (2011) 486–494.
[21] A. Apel, I. Herr, H. Schwarz, H.P. Rodemann, A. Mayer, Blocked autophagy sensitizes resistant carcinoma cells to radiation therapy, Cancer Res. 68 (2008) 1485–1494.
[22] N. Fujita, M. Hayashi-Nishino, H. Fukumoto, H. Omori, A. Yamamoto, T. Noda, T. Yoshimori, An ATG4B mutant hampers the lipidation of LC3 paralogues and causes defects in autophagosome closure, Mol. Biol. Cell 19 (2008) 4651–4659.
[23] S.K. Liu, S.A. Bham, E. Fokas, J. Beech, J. Im, S. Cho, A.L. Harris, R.J. Muschel, Delta-like ligand 4-notch blockade and tumor radiation response, J. Natl. Cancer Inst. 103 (2011) 1778–1798.
[24] A.K. Hadjantonakis, M. Gertsenstein, M. Ikawa, M. Okabe, A. Nagy, Generating green fluorescent mice by germline transmission of green fluorescent ES cells, Mech. Dev. 76 (1998) 79–90.
[25] S.S. Williams, T.R. Alosco, E. Mayhew, D.D. Lasic, F.J. Martin, R.B. Bankert, Arrest of human lung tumor xenograft growth in severe combined immunodeficient mice using doxorubicin encapsulated in sterically stabilized liposomes, Cancer Res. 53 (1993) 3964–3967.
[26] S. Shen, O. Kepp, M. Michaud, I. Martins, H. Minoux, D. Metivier, M.C. Maiuri, R.T. Kroemer, G. Kroemer, Association and dissociation of autophagy, apoptosis, and necrosis by systematic chemical study, Oncogene 30 (2011) 4544–4556.
[27] X. Ma, S. Piao, D.W. Wang, Q.W. McAfee, K.L. Nathanson, J.J. Lum, L.Z. Li, R. Amaravadi, Measurements of tumor cell autophagy predict invasiveness, resistance to chemotherapy, and survival in melanoma, Clin. Cancer Res. 17 (2011) 3478–3489.
[28] A.M. Wensing, N.M. van Maarseveen, M. Nijhuis, Fifteen years of HIV protease inhibitors: raising the barrier to resistance, Antiviral Res. 85 (2010) 59–74.
[29] M.C. Maiuri, E. Tasdemir, A. Criollo, E. Morselli, J.M. Vicencio, R. Carnuccio, G. Kroemer, Control of autophagy by oncogenes and tumor suppressor genes, Cell Death Differ. 16 (2009) 87–93.
[30] D.Y. Ouyang, L.H. Xu, X.H. He, Y.T. Zhang, L.H. Zeng, J.Y. Cai, S. Ren, Autophagy is differentially induced in prostate cancer LNCaP, DU145, and PC-3 cells via distinct splicing profiles of ATG5, Autophagy 9 (2013) 20–32.
[31] J.L. Webb, B. Ravikumar, D.C. Rubinsztein, Microtubule disruption inhibits autophagosome–lysosome fusion: implications for studying the roles of aggresomes in polyglutamine diseases, Int. J. Biochem. Cell Biol. 36 (2004) 2541–2550.
[32] S. Shen, O. Kepp, I. Martins, I. Vitale, S. Souquere, M. Castedo, G. Pierron, G. Kroemer, Defective autophagy associated with LC3 puncta in epothilone-resistant cancer cells, Cell Cycle 9 (2010) 377–383.
[33] K. Lee, D.Z. Qian, S. Rey, H. Wei, J.O. Liu, G.L. Semenza, Anthracycline chemotherapy inhibits HIF-1 transcriptional activity and tumor-induced mobilization of circulating angiogenic cells, Proc. Natl. Acad. Sci. U.S.A. 106 (2009) 2353–2358.
[34] R. Mathew, C.M. Karp, B. Beaudoin, N. Vuong, G. Chen, H.Y. Chen, K. Bray, A. Reddy, G. Bhanot, C. Gelinas, R.S. Dipaola, V. Karantza-Wadsworth, E. White, Autophagy suppresses tumorigenesis through elimination of p62, Cell 137 (2009) 1062–1075.